

A Machine Learning-Enabled mmID-Sensor for High-Accuracy Orientation and DoA Estimation

Marvin Joshi

*School of Electrical and Computer Engineering
Georgia Institute of Technology
Atlanta, GA, USA
mjoshi5@gatech.edu*

Charles Lynch

*School of Electrical and Computer Engineering
Georgia Institute of Technology
Atlanta, GA, USA
clynch19@gatech.edu*

Genaro Soto-Valle

*School of Electrical and Computer Engineering
Georgia Institute of Technology
Atlanta, GA, USA
genarosva@gatech.edu*

Manos Tentzeris

*School of Electrical and Computer Engineering
Georgia Institute of Technology
Atlanta, GA, USA
etentze@ece.gatech.edu*

Abstract—In this work, the implementation of a machine learning algorithm in conjunction with a Frequency-Modulated Continuous Wave (FMCW) radar system and a miniaturized ultra-low-power 24 GHz–mmID for precise localization, orientation sensing, and direction of arrival (DoA) estimation is presented. The rotational sensing capability is exploited by the use of four antenna elements with different polarization offsets between each other. The Multiple Signal Classifier (MUSIC) algorithm is employed for accurate DoA estimation, utilizing a single input multiple output (SIMO) custom antenna configuration on the reader system. The supervised learning KNN-model enabled achieving a high accuracy $< 1^\circ$ orientation detection along the z-axis, whereas the MUSIC algorithm achieved a mean error of $< 1^\circ$ in DoA estimation over a wide azimuth range of $\pm 45^\circ$, both at a range of 4m. The proposed system presents an important step for envisioning highly accurate virtual reality and motion-tracking systems in real time.

Index Terms—millimeter-Wave, RFID, Machine Learning, Radar, AR/VR, Localization

I. INTRODUCTION

In recent times, there has been an increasing interest in the development of virtual reality (VR) technologies, which has been pushed forward by other emerging trends including the Internet of Things (IoT), digital twins, Industry 4.0, and even telemedicine. In this regard, accurate localization sensing technologies are crucial for enabling the next generation of VR systems, and Radio Frequency Identification (RFID) systems have shown great potential for enabling them.

RFID technology – especially at UHF frequencies – has been widely used for decades in multiple commercial and industrial applications such as inventory management, security systems, logistics tracking, among others. The increased availability of 5G/mm-Wave systems has enabled RFID to extend to higher frequencies, supporting higher data rates, higher localization resolution and allowing to design more compact systems, overcoming some of the limitations of using UHF frequencies. This has made mm-Wave RFID (mmID) technology an excellent candidate for highly-accurate localization in

VR systems, however, it is still in the very early stages [1], [2].

The use of Frequency-Modulated Continuous Wave (FMCW) has become a popular approach for RFID tag localization, especially for mm-Wave RFIDs systems, as off-the-shelf FMCW radar systems are becoming more available and low-cost. In addition, machine learning (ML) algorithms have proved to enhance detection accuracy for different RFID systems where multiple data dimensions need to be analyzed, enabling applications such as precise human body tracking [3], precise multitarget localization [4], and enhanced chipless RFID detection [5].

In the context of VR and motion tracking scenarios, orientation and direction of arrival (DoA) estimation becomes crucial parameters for precise object tracking. Different works have reported different methods for orientation and DoA detection, demonstrating the ability to sense orientation and localization at the same time by utilizing multiple tags and/or multiple reader configurations [5], [6]. However, the use of UHF frequencies for these systems limits their spatial resolution and makes the overall system rather bulky. In this work, the integration of a miniaturized, ultra-low-power mmID system with ML algorithms is proposed to enable high-accuracy orientation detection as well as a angular estimation in the azimuth direction.

II. MMID TAG AND READER CONFIGURATION

A. Low-Power Gyro mmID Tag

The mmID tag utilized in this work for three-axes orientation detection has an operating frequency of 24.125 GHz and is composed of four antenna elements and the baseband circuitry, similar to the one presented in [2]. Each of the antenna elements was designed using a cross-polarized configuration to improve self-interference rejection, and they utilize a low-noise FET (CE3520K3, CEL) for load modulation. The baseband circuit consists of a 3V coin cell battery, a

1.8V regulator, and an ultra-low-power resistor-set voltage-controlled oscillator (LTC6903). The mmID tag has an overall miniaturized size of $43\text{ mm} \times 25\text{ mm}$ and was fabricated on RO4350B substrate ($\epsilon_r = 3.66, \tan \delta = 0.0037$), keeping a 6.5 mm separation ($\approx \lambda/2$) between each radiating element, as presented in Fig. 1a. Here, each element is labeled from A to D.

The rotation detection around the z-axis (Roll rotation, as shown in Fig. 1b) is enabled by the fact that, for a linearly-polarized interrogation, the angle offset of each element alters the polarization mismatch factor, which allows encoding of the rotation angle in the amplitude response of the backscattered signal. The use of four antenna elements with a polarization offset of 15° between each other allows tracking the amplitude change of each channel and to resolve angular ambiguities based on the different responses. Finally, the discrimination of each receiving channel is achieved by selecting different modulation frequencies for each element. These were selected so harmonic interference is avoided, so 49 kHz , 69 kHz , 85 kHz , and 110 kHz were chosen for elements A to D, respectively.

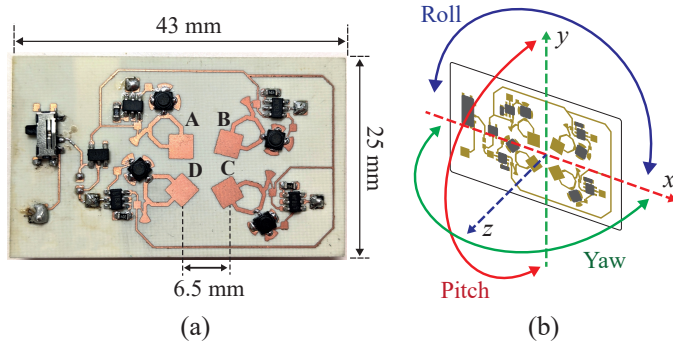


Fig. 1. (a) Fabricated mmID Gyro tag denoting its four antenna elements and baseband circuit components. (b) Diagram of rotational movements for each axis.

B. FMCW Reader System

The reader utilized in this work is the 24 GHz EVAL-RADAR-MMIC2 designed by Analog Devices. This FMCW radar is a low-cost, readily available chipset comprised of the ADF5901 24 GHz Tx MMIC, the ADF5904 24 GHz Rx MMIC, and the ADF4159 13 GHz PLL, which allows to synthesize a series of chirps for the mmID interrogation and to perform demodulation by mixing the transmitted and received signal. Each demodulated baseband signal is then sampled and visualized using the Tektronix DPO7354 Oscilloscope.

In order to support single input multiple output (SIMO) configuration, a custom-made cross-polarized antenna module composed of one transmitting element and four receiving elements was utilized. The Tx element is a single microstrip patch antenna, whereas each of the Rx elements consists of a series-fed linear patch antenna array separated by $\lambda/2$, achieving higher antenna gain. The antenna module was fabricated on RO4003 substrate ($\epsilon_r = 3.38, \tan \delta = 0.0027$), has a total size of $120\text{ mm} \times 67\text{ mm}$, and exhibits high Tx/Rx interference

isolation due to the cross-polarized configuration. The layout of the antenna module, as well as the reader schematic, are shown in Fig. 2.

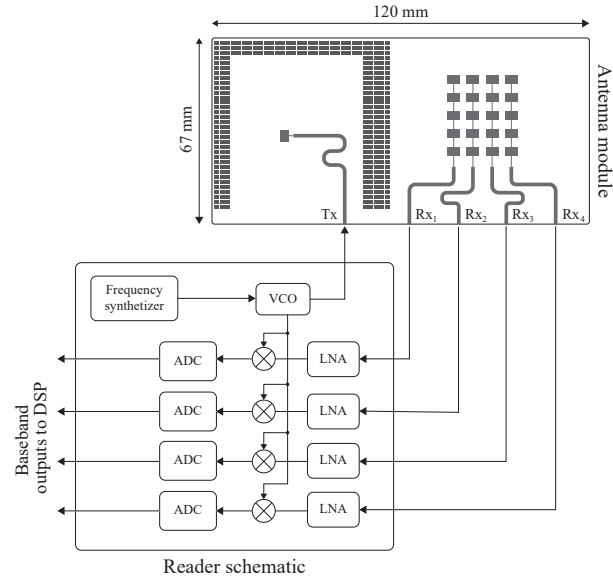


Fig. 2. Antenna module layout (top) and reader system schematic (bottom) utilized for mmID rotation and DoA detection.

III. SIGNAL PROCESSING FRAMEWORK

A. Tag Amplitude Detection

The radar was programmed to a triangular waveform with chirp period of 5 ms and frequency slope of $400\text{ MHz}/\mu\text{s}$. With the oscilloscope configured to a sampling rate of 500 kHz for 200 ms , this results in 19 complete triangular chirps. Each of the positive and negative ramps from the triangular waveform were processed separately, which results in 38 unique observations for each receive channel. The collected data from each receive channel was combined to form a radar cube, with dimensions of $\text{Samples} \times \text{Chirps} \times \text{Channels}$.

Fig. 3 summarizes the diagram of the processing chain. To visualize the tag from the baseband signals, a range Fast Fourier Transform (FFT) is performed across the Samples dimension of the radar cube. From the magnitude spectrum, the information from the tag can be seen. Fig. 4 is an example spectrum of the tag, where the modulation peaks of each element on the tag are shown, centered around their respective modulation frequency.

B. Direction of Arrival

With the use of a SIMO radar, direction of arrival (DoA) techniques can be implemented to determine the angular location of the tag in the azimuth direction. While popular methods, such as the Capon Beamforming and Bartlett Beamforming have been used for their low complexity and easy implementation, super resolution algorithms have been shown to provide higher accuracy [7]. These high-resolution algorithms fall into the approach of using subspace-based techniques. These techniques involve the use of eigen-decomposition to

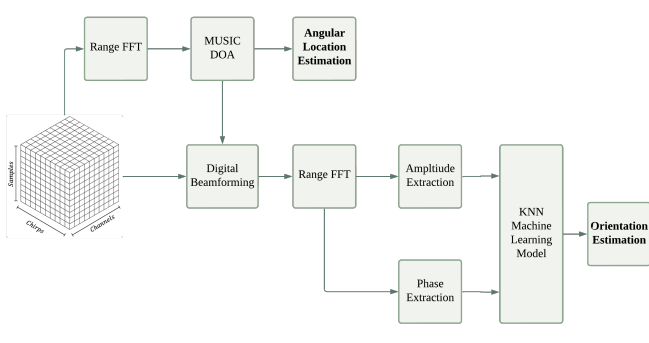


Fig. 3. Flow Chart of Signal Processing Chain

isolate noise and signal subspace [8]. The Multiple Signal Classifier (MUSIC) algorithm is one of the most widely used subspace-based methods [9]. The algorithm uses eigenvalue decomposition on the covariance matrix of the received signals, which results in two orthogonal subspaces, one in a noise subspace and the other in a signal subspace. Using these subspaces, a spectrum can be formed to estimate the DoA. First, the covariance matrix is calculated using (1), where S is the number of samples.

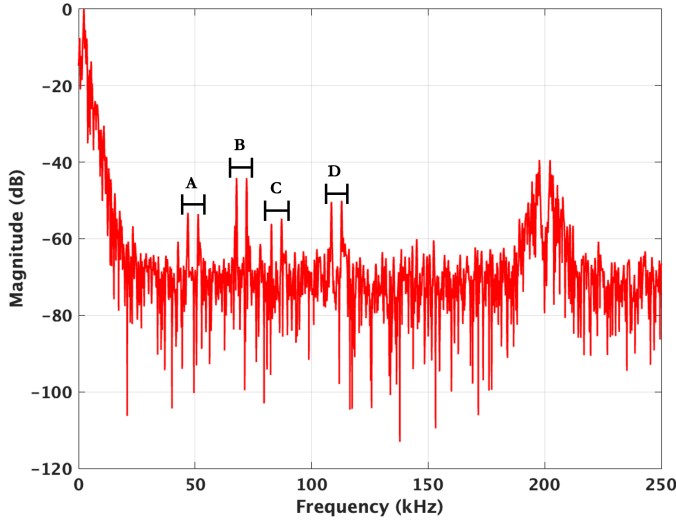


Fig. 4. Magnitude Spectrum of mmID Tag at Boresight

$$R_{xx} = \frac{1}{S} \sum_{n=0}^S x_n x_n^H \quad (1)$$

Next, the eigenvalue decomposition is performed on the covariance matrix and the eigenvalues are sorted from smallest to largest. Using these sorted eigenvalues, the eigenvectors are now sorted into signal and noise subspaces, Q_s and Q_n respectively. The pseudospectrum can now be formed using (2), where $a(\theta)$ is the steering vector.

$$P_{MUSIC}(\theta) = \frac{1}{a^H(\theta) Q_n Q_n^H a(\theta)} \quad (2)$$

While these algorithms are computationally longer, subspace base techniques allow for higher resolution and higher accuracy estimates [8].

C. Digital Beamforming

While beamforming has been primarily used for steering the beam of an antenna in a certain direction, adaptive digital beamforming methods have been shown to increase the SNR of a signal in a scene [10]. Beamforming can be applied to both transmitting and receiving elements, but for this work, only the received data will be beamformed. The effectiveness of a system's beamforming capabilities will primarily dependent on the total number of channels available in the system, and the accuracy of the DoA estimation methods. The beamformed data can be defined by (3), where $y(k)$ is the beamformed data, w_n is our weight vector, $x_n(k)$ is our radar cube and N is the number of channels [10].

$$y(k) = \sum_{n=0}^{N-1} w_n^* x_n(k) \quad (3)$$

Using the MUSIC DoA method, the angular location of the tag in the azimuth plane is found, with the estimated angle denoted as θ . For every angle, θ , found, a new w_n will need to be calculated, and subsequently apply them to our original radar cube, $x(k)$, resulting in $y_m(k)$ where $m = 1 - M$ and M is the number of subjects. The FMCW radar used in these experiments contains one transmitter and four receivers, which results in four virtual channels. The four virtual channels form a linear array with a spacing of half-wavelength. Using this information, the weight vector, w_n , can be calculated as shown in (4), where k_0 is the free-space wavenumber and d is the spacing between channels. Given our special case where $d = \frac{\lambda}{2}$, the weight vector can be further simplified to become (5). In Fig. 5, the beamforming process is summarized, and it shows how the weights will be applied to each channel.

$$w_n = e^{-jk_0 d n \cos \theta} \quad (4)$$

$$w_n = e^{-j\pi n \cos \theta} \quad (5)$$

D. Phase Extraction

Using the beamformed data, a range FFT is again performed to decode the tag. Utilizing a custom peak detection algorithm, the modulating beat frequencies of each element can be identified, which allows for the extraction of the phase difference of the antenna elements on the tag. It has been previously shown that the localization using the phase difference of two receiving antennas has provided higher accuracy at farther ranges when compared to techniques utilizing just received signal strength [11]. The Arctangent Demodulation algorithm is a phase based method used to extract the phase of I/Q Signals. This algorithm determines the phase angle of the radar signal and prevents large phase drift with the use of phase unwrapping [12]. With the mmID comprised of 4 antenna elements, the phase difference of neighboring elements, i.e elements B-A, C-B, D-C and A-D, are calculated.

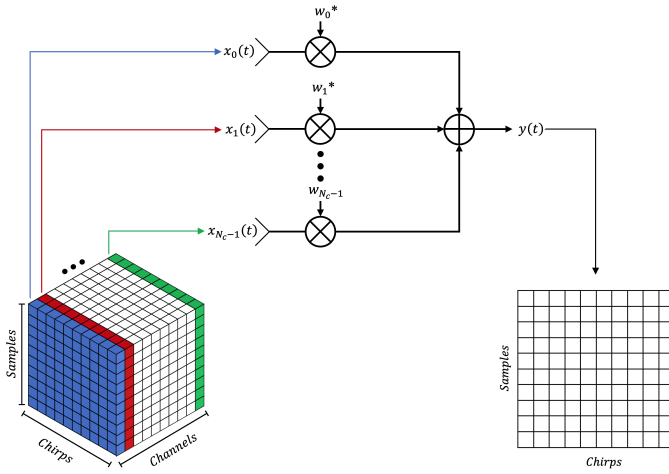


Fig. 5. Digital Beamforming of Radar Cube

E. Machine Learning Model

In this work, a K-Nearest Neighbors (KNN) machine learning algorithm is used to train and predict the orientation of the tag. The KNN algorithm is distance-based, where it classifies, or groups, a given data point to observations that are the most similar. This makes the KNN network an ideal model for this work. The model uses the amplitude response of each element on the tag, along with the phase difference from the neighboring elements, i.e. elements B-A, C-B, D-C and A-D, as inputs.

IV. EXPERIMENTAL SETUP AND RESULTS

A. Direction of Arrival Estimation

Various tests are performed to display the capabilities of the mmID tag. A visualization of the measurement setup can be found in Fig. 6. In the first set of experiments, the angular localization ability was investigated. The tag is placed on a 3-Axis Gimbal Holder at a radial distance, R , from the front of the reader's antenna. While keeping the radial distance

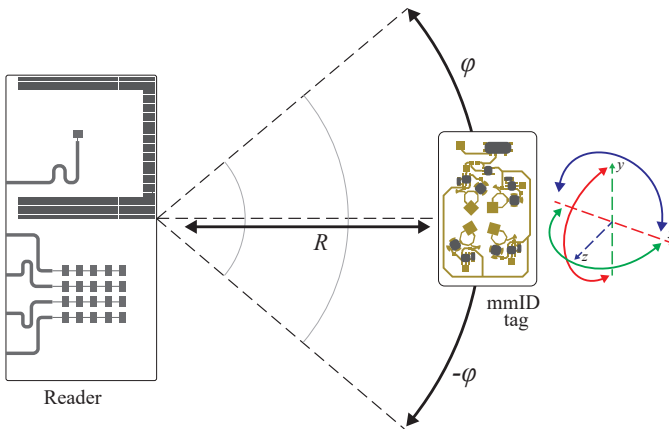


Fig. 6. Measurement setup for DoA and orientation detection. The mmID tag was measured at different ranges, R , and different azimuth angles, φ .

constant, the mmID was moved from $\pm 45^\circ$ in steps of 5° . This measurement was performed at radial distances of 1 – 4 m, with steps of 1 m. Utilizing 2^{10} data samples, the results from these measurements can be found in Table I. It can be seen that while the angular estimation does increase across the different ranges, utilizing the MUSIC algorithm has allowed for the error to remain below 1° . Fig. 7 shows the results from the 4 m scenario, where the estimated angles match well with the ground truth.

TABLE I
DOA ESTIMATED MEASUREMENT RESULTS

Range	MUSIC Mean φ error
1 m	0.157°
2 m	0.211°
3 m	0.632°
4 m	0.947°

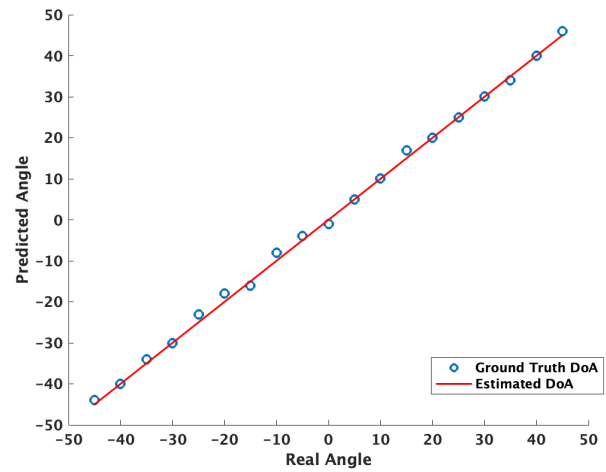


Fig. 7. Predicted vs. Real DoA Estimation at 4 m

B. Tag Orientation Estimation

The next set of measurements were to determine the ability to extract the orientation of the tag. The tag was mounted on a 3-Axis Gimbal and placed at boresight at a distance, R , in front of the radar. While holding the Yaw and Pitch axes, the mmID was rotated along the Roll axis in 1° steps over an angular range of $\pm 90^\circ$. The measurements were performed at distances of 1 – 4 m, with steps of 1 m. With 38 observations taken per each rotation angle, a global data set of 27,512 unique observations was formed. The dataset was then split into 80% for training and 20% for testing the model. The results from the KNN Model can be found in Table II. The table shows high accuracy in detecting the orientation angle, as the maximum mean orientation error was only 0.1043° at a distance of 4 m. The results from the 4 m experiment can be found in Fig. 8. Confirming the results of the table, it can be seen that near zero orientation error was achieved.

TABLE II
ACCURACY AND MEAN ERROR PERFORMANCE OF KNN MODEL AT
DIFFERENT TEST RANGES

Range	KNN Model Accuracy	Mean Orientation Error
1 m	99.21%	0.0284°
2 m	97.97%	0.0775°
3 m	94.59%	0.0672°
4 m	93.06%	0.1043°

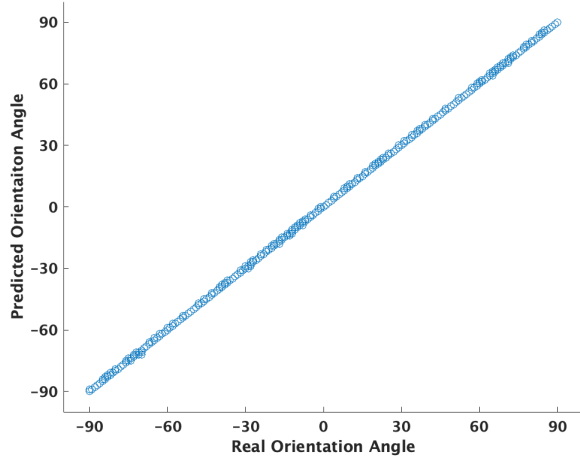


Fig. 8. Predicted Orientation vs. Real Orientation in Roll Axis at Distance = 4 m

V. CONCLUSION

In this work, the authors have proposed the utilization of a simple and robust KNN machine learning algorithm in combination with an FMCW reader and an ultra-low-power 24 GHz–mmID tag for high-accuracy rotational sensing and DoA estimation. The MUSIC algorithm was employed for DoA estimation, which allowed to obtain a mean error of less than 1° in azimuth direction at a 4 m range. Moreover, the KNN model achieved an accuracy of 93.06% in orientation detection at the same range, with an error of only 0.1°. The system has great potential for applications in augmented reality, motion capture, and accurate object tracking, where fine spatial resolution is crucial for mapping real-world objects into the digital world, enabling very low-cost and highly-scalable tracking systems.

REFERENCES

- [1] R. Xiao, A. Vianto, A. Shaikh, O. Buruk, J. Hamari, and J. Virkki, "Exploring the application of rfid for designing augmented virtual reality experience," *IEEE Access*, vol. 10, pp. 96 840–96 851, 2022.
- [2] A. Adeyeye, C. Lynch, J. Hester, and M. Tentzeris, "A machine learning enabled mmwave rfid for rotational sensing in human gesture recognition and motion capture applications," in *2022 IEEE/MTT-S International Microwave Symposium - IMS 2022*, 2022, pp. 137–140.
- [3] G. A. Oguntala, R. A. Abd-Alhameed, N. T. Ali, Y.-F. Hu, J. M. Noras, N. N. Eya, I. Elfergani, and J. Rodriguez, "Smartwall: Novel rfid-enabled ambient human activity recognition using machine learning for unobtrusive health monitoring," *IEEE Access*, vol. 7, pp. 68 022–68 033, 2019.

- [4] Y. Ma, B. Wang, X. Gao, and W. Ning, "The gray analysis and machine learning for device-free multitarget localization in passive uhf rfid environments," *IEEE Transactions on Industrial Informatics*, vol. 16, no. 2, pp. 802–813, 2020.
- [5] Z. Wang, M. Xu, and F. Xiao, "Recognizing 3d orientation of a two-rfid-tag labeled object in multipath environments using deep transfer learning," in *2021 IEEE 41st International Conference on Distributed Computing Systems (ICDCS)*, 2021, pp. 652–662.
- [6] M. B. Akbar, C. Qi, M. Alhassoun, and G. D. Durgin, "Orientation sensing using backscattered phase from multi-antenna tag at 5.8 ghz," in *2016 IEEE International Conference on RFID (RFID)*, 2016, pp. 1–8.
- [7] V. Krishnaveni, T. Kesavamurthy, and B. Aparna, "Beamforming for direction-of-arrival (doa) estimation-a survey," *International Journal of Computer Applications*, vol. 61, pp. 4–11, 2013.
- [8] F. Akbari, S. Shirvani Moghaddam, and V. Tabataba Vakili, "Music and mvdr doa estimation algorithms with higher resolution and accuracy," in *2010 5th International Symposium on Telecommunications*, 2010, pp. 76–81.
- [9] R. K and P. K. N, "Performance evaluation analysis of direction of arrival estimation algorithms using ula," in *2018 International Conference on Electrical, Electronics, Communication, Computer, and Optimization Techniques (ICEECCOT)*, 2018, pp. 1467–1473.
- [10] B. Van Veen and K. Buckley, "Beamforming: a versatile approach to spatial filtering," *IEEE ASSP Magazine*, vol. 5, no. 2, pp. 4–24, 1988.
- [11] C. Hekimian-Williams, B. Grant, X. Liu, Z. Zhang, and P. Kumar, "Accurate localization of rfid tags using phase difference," in *2010 IEEE International Conference on RFID (IEEE RFID 2010)*, 2010, pp. 89–96.
- [12] B.-K. Park, O. Boric-Lubecke, and V. M. Lubecke, "Arctangent demodulation with dc offset compensation in quadrature doppler radar receiver systems," *IEEE Transactions on Microwave Theory and Techniques*, vol. 55, no. 5, pp. 1073–1079, 2007.